

Laser-induced acoustic phonon gratings in semiconductor thin films

J. Wang, D. C. Hutchings,^{a)} A. Miller,^{b)} and E. W. Van Stryland^{b)}
Center for Research in Electro-optics and Lasers, University of Central Florida, Orlando, Florida 32826

K. R. Welford, I. T. Muirhead,^{c)} and K. L. Lewis
Defense Research Agency, Great Malvern, Worcs. WR14 3PS, United Kingdom

(Received 10 August 1992; accepted for publication 19 January 1993)

Laser induced ultrasonic standing waves are observed in molecular beam deposited ZnSe thin films using the transient grating technique. This observation is attributed to a very short trapping time for single photon absorption in the band tail. The period of the standing wave is used to determine the acoustic phonon velocity in the ZnSe thin film which indicates that it is longitudinal acoustic phonons which are excited.

I. INTRODUCTION

Laser induced ultrasonic waves¹⁻³ have been observed and studied in liquids,⁴ molecular solids,^{1,2} and superconducting thin films⁵ using the transient grating method. The technique uses two time-coincident laser pulses to create an optical interference pattern in the medium. Energy is then transferred to the material by optical absorption or Brillouin scattering, which results in the launching of counter-propagating ultrasonic waves with a wavelength matching that of the original grating. This leads to a standing wave pattern whose oscillations can be probed with an additional time delayed probe pulse. By varying the grating spacing, (by changing the angle between the incident pulses) the acoustic frequency can be continuously tuned. This technique is also referred to as laser-induced phonon spectroscopy (LIPS)³ as it provides a probe of the phonon dispersion.

Coherent acoustic phonon gratings are not observed in bulk semiconductors under normal conditions because optically excited excess carriers usually have (a) relatively long recombination times and (b) high mobilities allowing them to diffuse significant distances before recombining. Either of these effects will inhibit the creation of oscillating ultrasonic standing waves. Acoustic phonons are created in semiconductors from the energy dissipated in nonradiative carrier recombination. In order to produce the necessary coherence of the phonons which will result in an oscillating standing wave (a) carrier diffusion must be restricted to avoid washing out of the grating, and (b) the energy transfer to the lattice must occur on a time scale shorter than the phonon period. When both of these conditions are satisfied a modulating diffracted signal should be observed by the transient grating technique due to the beating of counter-propagating acoustic waves.

In this article we describe the optical generation and detection of acoustic phonon modes in a semiconductor using the transient grating method. The appropriate conditions are created by employing a film of ZnSe microcrys-

tallites with sizes much less than the grating period. Molecular beam deposited (MBD) films of thickness sufficient to allow efficient diffraction of picosecond pulses are used to time resolve the dynamics of the phonon grating. This provides a noncontact method of determining the acoustic phonon velocities.

II. BACKGROUND

The transient grating method is a technique frequently used for measuring and determining the dynamics of optical nonlinearities. Basically, a grating is formed by interfering two coherent light beams on a sample.⁶ This can be accomplished with the two beams incident on the same or opposite sides of the sample. The grating may even be derived from one beam if there is some back reflection within or external to the sample. The optical nonlinearity in the sample results in a corresponding grating modulation in either or both the refractive index and absorption coefficient. This grating in the optical constants can cause the diffraction of a light beam which can be a separate beam or one of those that write the grating (self-diffraction). The amount of diffracted light depends on the grating amplitude and so is a direct measure of the magnitude of the optical nonlinearity (although it gives no information regarding the sign of the nonlinearity). Diffraction from refractive gratings is more commonly observed as efficiencies are typically higher than for absorptive gratings.

In the three beam configuration, if the beam that reads the grating is time delayed, this technique becomes a powerful method for observing the dynamics of optical nonlinearities. For example, by measuring the decay of a carrier induced grating in semiconductors, information can be obtained about carrier diffusion and recombination.⁷

One of the applications of the transient grating technique is laser-induced phonon spectroscopy.³ Here, the optical energy in the grating is transferred into coherent phonons (usually longitudinal) whose wavelength matches that of the optical grating. The mechanism by which these coherent phonons are generated generally depends on whether the sample is optically absorbing or transparent at the laser wavelength. If the sample is absorbing (into vibrational or electronic states) and there is a rapid radi-

^{a)}Present address: Dept. of Electronics and Electrical Engineering, Univ. of Glasgow, Glasgow G12 8QQ, U.K.

^{b)}Also with the Departments of Physics and Electrical Engineering, Univ. of Central Florida, FL.

^{c)}Present address: OCLI, Dunfermline, KY11 5JE, Scotland.

tionless relaxation, there will be local heating at the grating maxima. Thermal expansion then causes the net movement of atoms or molecules away from the interference maxima towards the minima thus setting up the counterpropagating ultrasonic waves. The alternative mechanism for non-absorbing media is that optical energy can be coupled directly into coherent phonons by stimulated Brillouin scattering. Here a photon from one of the writing beams is scattered to create an acoustic phonon and a lower energy photon in the other beam (though still within the spectral bandwidth of the picosecond pulse). The same process also occurs for the other writing beam with the phonon having the opposite wave vector to the first and thus setting up counterpropagating ultrasonic waves. Experimentally, these two mechanisms can be differentiated by the time response with the thermal mechanism giving one diffraction maximum per acoustic cycle and the stimulated Brillouin mechanism giving two diffraction maxima per cycle.³ It should be noted though that in both cases the diffraction signal will be at a minimum at the instant the grating is written and then increase as the material is displaced and strain is induced.

Coherent phonon oscillations have also been optically detected using the excite-probe method with femtosecond pulses in GaAs,⁸ single crystals of Sb, Bi, Te and Ti₂O₃,⁹ and thin-film YBa₂Cu₃O_{6+x},¹⁰ where the excite pulse acts as an impulse and the probe detects the "ringing" of the lattice. This technique generally excites optical phonon modes, hence the requirement that the optical pulses be less than a phonon period means that optical pulses typically have to be less than 100 fs in duration.

Absorption of light of wavelengths close to the band edge in semiconductors can lead to a change in the optical properties usually through free-carrier or thermal effects. The excitation of electrons from valence to conduction band can change the optical properties, e.g., by inhibiting further transitions or phenomena associated with the change in conductivity (e.g., photorefractive effect, self-electro-optic effect devices). For wavelengths longer than the fundamental absorption edge in semiconductors, free-carrier effects normally give rise to a reduction in the refractive index. Thermal expansion leads to an increasing band gap with temperature whereas changing the phonon population leads to a decreasing band gap with temperature.¹¹ In most semiconductors it is the latter of these effects which dominates and the band gap decreases with increasing temperature giving an increase in the refractive index.

III. EXPERIMENT

The samples used in this experiment are ZnSe thin films of thickness 5 μm grown by molecular beam deposition on glass substrates.¹² This method was developed for the growth of high quality, high density optical coatings.

Films were grown in a Vacuum Generators load-locked ultrahigh vacuum system fitted with Knudsen sources and *in situ* surface diagnostics. The zinc selenide source was ultrahigh purity polycrystalline ZnSe which had previously been prepared by chemical vapor deposition

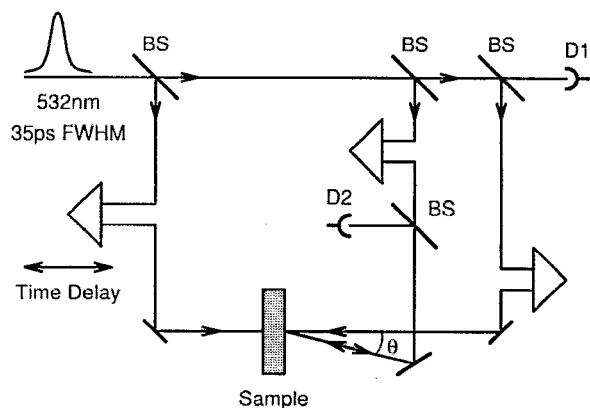


FIG. 1. Standard backward degenerate-four-wave-mixing setup. The forward pump and probe pulses are time coincident on the sample and create a grating which is probed by a variably time delayed backward pump pulse.

from a mixture of zinc vapor and hydrogen selenide. The source material was contained within a high purity graphite crucible which was carefully outgassed following baking of the entire deposition chamber at 180 °C. The deposition process allows the deposition of films with a high degree of perfection. Thick films could be produced which do not delaminate from the substrate and which have a high degree of optical stability as a consequence of lack of open porosity. Interference filters grown by this technique have been used in optical bistability experiments and show higher stability than those produced by more conventional techniques.¹³

MBD ZnSe films on glass substrates show extremely low photoluminescence efficiencies indicating that the primary relaxation of the carriers occurs through traps. This implies a very short relaxation time for the carriers. Time resolved photoluminescence studies in this type of material confirm this with no photoluminescence being visible on a time resolution of 10 ps.¹⁴

Three samples were used in the present experiment. These were grown at substrate temperatures of 20, 100, and 300 °C. Cross-sectional transmission electron micrographs indicate a dense columnar polycrystalline structure with the columns growing perpendicular to the surface and having a length equal to the film thickness. Higher substrate temperatures produce larger microcrystalline diameters. Crystallite diameters measured for MBD ZnSe on GaAs are ~ 25 nm for room temperature growth and ~ 100 nm for a growth temperature of 190 °C.¹² Similar measurements for MBD ZnSe on glass are unavailable due to the inability to cleave the sample but microcrystalline diameters are not anticipated to be much larger than those grown on GaAs.

The experimental geometry is the standard backward degenerate-four-wave-mixing geometry as shown in Fig. 1. The input pulses are at a wavelength of $\lambda = 0.532 \mu\text{m}$ produced by frequency doubling a Q-switched mode-locked Nd:YAG laser (Quantel model YG401C) with a single pulse switched out at a repetition rate 10 Hz. The pulse width, which was deduced from an autocorrelation of the

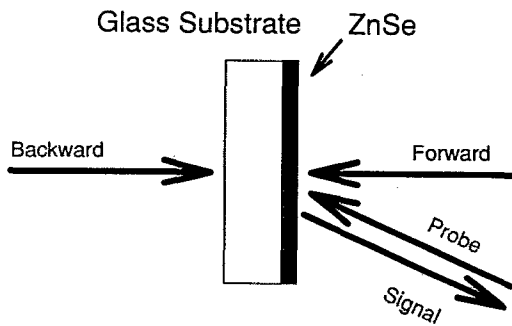


FIG. 2. Sample geometry. The time coincident forward pump and probe pulse writes a transverse grating in the ZnSe film which is read by the time delayed backward pump incident through the substrate.

fundamental pulses, was 35 ps full width at half-maximum (FWHM). The spatial profile of the pulses consisted of a single transverse mode of Gaussian form. In this experimental setup, the $0.532 \mu\text{m}$ pulses are split into three separate pulses; forward pump, backward pump, and probe. All three pulses pass through separate delay stages which can be adjusted to ensure the forward pump and probe are temporally coincident and all three pulses are spatially coincident at the sample. The backward pump and forward pump are counterpropagating with approximately the same energy. The probe enters the sample at an angle with respect to the forward pump, with 5% of the backward pump energy (Fig. 2). The beam radii ($1/e^2$ irradiance) at the sample position are 0.73 mm for the backward pump, 0.61 mm for the forward pump, and 0.43 mm for the probe. Typical energies for the backward pump pulses were around $150 \mu\text{J}$ (corresponding to a peak irradiance of 0.47 GW/cm^2). The two time-coincident laser pulses (forward pump and probe) are crossed inside the sample to setup an optical interference pattern with grating period

$$\Lambda = \frac{\lambda}{2n \sin(\theta/2)}, \quad (1)$$

where n is the linear refractive index of the material and θ the angle between forward pump and probe beams inside the material. By altering the angle between the forward pump and probe beams, the grating spacing can be adjusted. If some nonlinear mechanism exists in the material whereby intense light causes a change in the optical properties of the material, the backward pump will experience diffraction into the counterpropagating direction of the probe beam. The dependence of the diffracted signal strength on delay allows a measurement of the decay of the grating modulation.

Each data point is an average of ten shots, taken automatically by computer. While taking the data, the pulse width and amplitude are also monitored and windows of $\pm 5\%$ have been set for both pulse width and energy in order to increase the signal to noise level. The signals are detected by integrating silicon photodiodes with a peak sample and hold circuitry. A calcite polarizer and half-wave plate were used to adjust the total input energy.

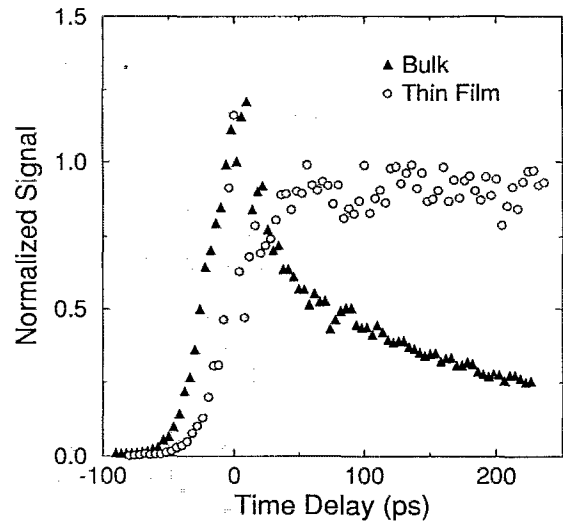


FIG. 3. Comparison of the diffracted signal as a function of time delay (up to 200 ps) for bulk polycrystalline and MBD thin film ZnSe.

IV. RESULTS

Figure 3 shows a comparison of the time response of the diffracted signal obtained from a MBD thin film ZnSe sample to that obtained in bulk polycrystalline ZnSe using the same experimental setup. The diffracted signal from bulk ZnSe shows a peak at zero delay which is the auto-correlation of the laser pulse attributed to the combined effects of the instantaneous bound electronic nonlinear refraction n_2^{15} and two photon absorption. This is followed by an exponentially decaying tail arising from the refractive index change associated with bandfilling by free carriers generated by two-photon absorption.¹⁶ The decay time of the tail is set by a combination of recombination and ambipolar diffusion of the free carriers washing out the grating.

In contrast, the diffracted signal from the thin film of ZnSe is basically an integration of the input pulse and shows no signs of decay on comparable time scales (< 200 ps). There is some evidence of a coherence spike at zero delay which is due to self-diffraction of the backward pump from the grating produced by this pulse and the probe pulse. This may arise from the free electronic contribution to the nonlinearity but needs further investigation.

The lack of an observed decay on these time scales is consistent with a thermal grating. The absorption tail at the band edge is quite extensive in the thin film MBD ZnSe¹³ and a substantial density of free carriers can be generated by single photon absorption at 532 nm. These carriers become trapped on time scales on the order of or less than the pulse width as indicated by photoluminescence studies.

The grating modulation is generated along the thin film and so if carrier diffusion were to wash out the grating, it would need to be in a direction perpendicular to the crystallite columns. Using a diffusion coefficient of $4.5 \text{ cm}^2/\text{s}$ for ZnSe¹⁶ gives a time scale of around a picosecond for the carriers to reach a 25 nm microcrystallite boundary.

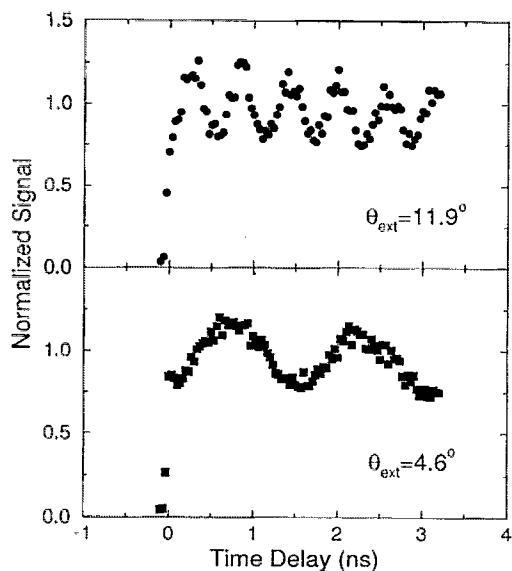


FIG. 4. Diffraction signal as a function of time delay (up to 3 ns) in MBD thin film ZnSe for two different external angles between the forward pump and probe beams as indicated. Changing the external angle results in a variation in the grating spacing and so varies the wave vector of the excited phonon mode.

The crystallite column diameters are much smaller than the grating spacings employed. The trapping of the carriers in defects at these boundaries is consistent with experimental observation. The excess energy of the electrons is all deposited as heat to produce a thermal grating.

The diffracted signal from the thin film MBD ZnSe on longer time scales is shown in Fig. 4 for two different grating spacings using the sample grown at 300 °C. These signals show an oscillating signal superimposed on a background which may show some signs of a slow decay. The period of the oscillation is 1.65 ns for an external input angle of 4.6° (corresponding to a grating spacing of $\Lambda = 6.6 \mu\text{m}$) and 0.60 ns for an external input angle of 11.9° ($\Lambda = 2.6 \mu\text{m}$). The ratio of the magnitude of the oscillation to the background signal seems to be independent of angle. Similar data is obtained for samples corresponding to different growth temperatures Fig. 5 indicating there is no dependence on the microcrystalline diameter (at least in the limit where the diameter is much smaller than the grating spacing).

The oscillating diffraction signal results from an ultrasonic standing wave which is set up in the film (laser induced phonon grating).³ The transfer of energy to the lattice is spatially inhomogeneous, matching the original sinusoidal optical interference pattern. Thus the atoms will be more energetic at the grating peaks causing a net movement of the atoms from the grating peaks to the troughs. This movement results in the initiation of two counter-propagating sound waves which can also be described in terms of a standing wave.¹ This standing wave has exactly the same spatial separation as the original light grating from the interference of the forward pump and probe beams. The fact that the coherence of this ultrasonic standing wave is so evident indicates that energy is transferred

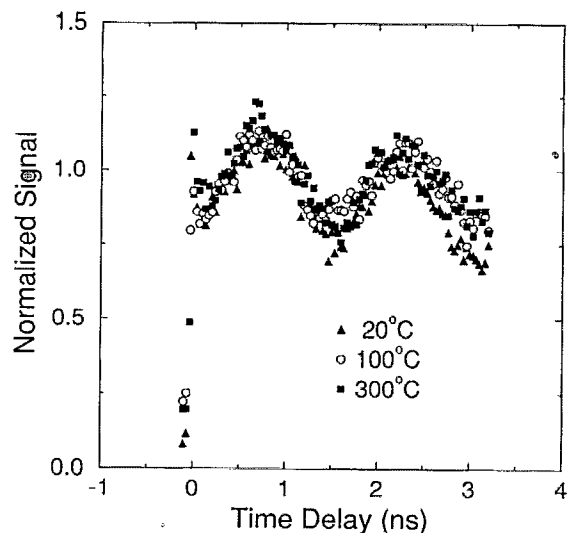


FIG. 5. Diffraction signal as a function of time delay for three different MBD thin film ZnSe samples grown at the different substrate temperatures indicated. The signal shows no dependence on the growth conditions.

from the excited carriers to the lattice on very short time scales (certainly much shorter than the oscillation period).

The period of the oscillation can be used to determine the speed of sound along the ZnSe thin film given that the grating spacing is known. For the 4.6° external angle measurement this gives the speed of sound as $v = 4000 \text{ m/s}$ and for the 11.9° external angle measurement, $v = 4300 \text{ m/s}$. These results are summarized in Table I. These measurements are in agreement with tabulated values for longitudinal acoustic phonon velocities in bulk ZnSe which lie in the range 4000–4600 m/s.¹⁷ This is to be contrasted with the reported observation of coherent longitudinal optical phonons in GaAs using a femtosecond excite-probe technique.⁸

The slowly decaying background signal is due to diffraction from a refractive grating associated with the thermal grating. This can be considered as an incoherent phonon effect. Most semiconductors have a positive $\partial n / \partial T$ at frequencies in the vicinity of the band edge including bulk and thin film ZnSe,¹³ hence the grating consists of an increase in refractive index. The energy for the temperature rise is also obtained from the release of energy from the optically excited carriers. The time evolution of the carrier density N and temperature rise ΔT is described using the coupled partial differential equations

TABLE I. Summary of the data on the two different grating spacings examined. For the external angles indicated, the grating spacing was calculated from Eq. (1), the period is from the observed oscillation in the time-delayed diffracted signal from which the speed of sound is inferred.

θ_{ext}	Λ	Period	Acoustic velocity
4.6°	6.6 μm	1.65 ns	4000 m/s
11.9°	2.6 μm	0.60 ns	4300 m/s

$$\frac{\partial N}{\partial t} = -\frac{N}{\tau_r}, \quad (2)$$

$$\frac{\partial(\Delta T)}{\partial t} = \frac{1}{\rho c} \left[\kappa \nabla^2(\Delta T) + \frac{E_r N}{\tau_r} \right], \quad (3)$$

with the initial conditions $\Delta T(t=0)=0$ and $N(t=0) = N_0 \sin^2(\pi x/\Lambda)$. The solution of this is

$$\Delta T = T_0(1 - e^{-t/\tau_r}) + T_0 \frac{(e^{-t/\tau_r} - e^{-t/\tau_{td}})}{(1 - \tau_r/\tau_{td})} \cos\left(\frac{2\pi x}{\Lambda}\right), \quad (4)$$

where the thermal time constant τ_{td} is given by

$$\tau_{td} = \frac{\rho c \Lambda^2}{4\pi^2 \kappa}, \quad (5)$$

and we define $T_0 = 2E_r N_0 / \rho c$. The recombination of the carriers occurs with a time constant τ_r and releases a quantity of energy E_r per carrier to the lattice. ρ , c , and κ are the density, specific heat capacity, and thermal conductivity, respectively, which for bulk polycrystalline ZnSe at room temperature are tabulated as $\rho = 5.27 \text{ g/cm}^3$, $c = 0.081 \text{ cal/(g }^\circ\text{C)}$, and $\kappa = 0.043 \text{ cal/(cm s }^\circ\text{C)}$.¹⁸

The observed decay of the background signal will depend on the recombination of the trapped carriers and thermal diffusion washing out the grating. It can be seen in Fig. 4 that the relative contribution to the diffraction efficiency from the ultrasonic standing wave does not depend on the grating spacing. Since the thermal diffusion time constant τ_{td} is proportional to the square of the grating spacing [Eq. (5)], and the temperature modulation of the grating is proportional to (and so the diffraction efficiency is dependent on) the quantity $(1 - \tau_r/\tau_{td})^{-1}$ [Eq. (4)], it can be concluded that $\tau_{td} \gg \tau_r$ and the observed decay of the thermal grating is completely dominated by thermal diffusion. Hence, Eq. (4) can be simplified to

$$\Delta T = T_0 \left[(1 - e^{-t/\tau_r}) + e^{-t/\tau_{td}} \cos\left(\frac{2\pi x}{\Lambda}\right) \right]. \quad (6)$$

Using the above constants for bulk ZnSe gives thermal time constants τ_{td} of 120 and 17 ns for our two grating spacings using Eq. (5), which is consistent with the experimental observations although the limited delay times prevent an accurate estimation of these time constants. This simplified analysis is for a bulk material (of infinite extent) with no net heat diffusion in the beam propagation direction. Obviously this is not quite the case for a thin film on a glass substrate. However, as the ZnSe thermal conductivity is much larger than for the glass, and the film thickness is of the same order as the grating spacing, it will be the direct transverse route along the film that dominates the decay of the thermal grating rather than any route for the heat diffusion through the glass substrate. Hence, this simplified model is reasonable.

It can be seen from Fig. 4 that the oscillating and background components of the diffraction signal combine together in such a fashion that the overall diffraction efficiency shows an initial increase. It has already been noted that the background (thermal) component is associated

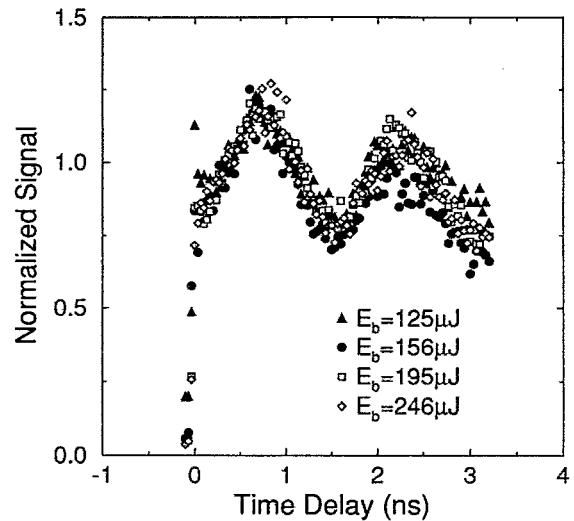


FIG. 6. Diffraction signal as a function of time delay for four different optical energy levels as shown. The optical power level is varied before the beam splitters and so is equally varied in all three beams. The signal is normalized by dividing by the cube of the relative optical input energy. As the normalized signal is identical in all four cases it can be concluded that no saturation of the nonlinearity is evident at these pulse energies.

with a refractive index increase. The observed form of the signal could arise with the oscillating component initially at a minimum and also giving an increase in refractive index. This can be attributed to the atoms being initially equidistant but as they move due to thermal expansion (thereby launching the standing longitudinal acoustic wave), the resulting larger spacing at the grating maximum gives a refractive index increase (and smaller spacing at the minimum gives a decreased refractive index). It should be noted though that the same form of signal could arise if the oscillating component has opposite sign but is initially at a maximum.

To check if the nonlinearity shows any saturation effects (i.e., shows the same power dependence as a third order nonlinearity), the input energy was varied. Figure 6 shows the normalized diffraction signal against the delay time of the backward pump. The normalization process involves dividing the diffraction efficiency by the input energy cubed since the input energy is adjusted before the beam splitters which maintain a constant energy ratio between the three beams. As the normalized signals are identical, it can be concluded that both the coherent phonon process and the background thermal grating show the same power dependence as a third order nonlinearity with no indication of saturation. Hence, over these optical energy ranges the refractive index change is directly proportional to the optical energy. This implies that the carrier density generated is proportional to the optical energy, the transfer of energy from carriers to acoustic phonons is density independent and shows no saturation of the traps, and the resulting temperature rise is small enough to give a linear dependence of the refractive index on temperature.

V. CONCLUSIONS

Transient grating measurements were performed on high quality MBD ZnSe films on glass substrates. Using 35 ps pulses at near band gap resonance no evidence of free-carrier induced optical nonlinearities were observed. This is attributable to fast trapping of the photogenerated carriers at the boundaries of the microcrystallites. This process results in a rapid transfer of energy into the lattice such that a coherent ultrasonic standing wave is produced. While the same phenomena has been observed in various media, it is rare for it to be observed in semiconductors since ambipolar carrier diffusion usually washes out the excitation grating before the energy is transferred to the lattice.

This LIPS technique provides a noncontact means of determining the acoustic phonon dispersion. At present only the acoustic velocity has been determined for the thin film ZnSe but similar measurements using longer time scales and shorter grating spacings may allow a more detailed determination of the acoustic phonon dispersion curve.

It is interesting to speculate whether the same technique could be applied to other semiconductors. Certainly thermo-optic coefficients in the vicinity of the band edge of most semiconductors are of comparable magnitude. It would be necessary to prevent the diffusion of energy before it is transferred to the lattice. This should be possible by introducing a higher density of impurities or defects to reduce the free-carrier relaxation time. This reduction in relaxation time has been demonstrated by ion-bombardment¹⁹ and by low temperature molecular beam epitaxial growth.²⁰ It also may be possible to use quantum well material in a geometry where the wells are parallel to the grating. Another approach may be to highly excite the carriers given that electrons and holes thermalize with the lattice on a time scale typically of a few picoseconds and this excess energy could result in a LIPS signal superimposed on the usual carrier induced diffraction signal. How-

ever, as the carriers would be excited well into the band, absorption coefficients would be high necessitating the use of thin film samples.

ACKNOWLEDGMENTS

We acknowledge the Defense Advance Research Projects Agency for support of this research and the collaboration between CREOL and DRA (Malvern). We thank D. J. Hagan for valuable discussions.

- ¹K. A. Nelson, D. R. Lutz, M. D. Fayer, and L. Madison, *Phys. Rev. B* **24**, 3261 (1981).
- ²K. A. Nelson, R. Casalegno, R. J. Dwayne Miller, and M. D. Fayer, *J. Chem. Phys.* **77**, 1144 (1982).
- ³M. D. Fayer, *IEEE J. Quantum Electron.* **QE-22**, 1437 (1986).
- ⁴G. Eyring and M. D. Fayer, *J. Chem. Phys.* **81**, 4314 (1984).
- ⁵C. D. Marshall, I. M. Fishman, and M. D. Fayer, *Phys. Rev. B* **43**, 2696 (1991).
- ⁶H. J. Eichler, *Opt. Acta* **24**, 631 (1977).
- ⁷H. J. Eichler and F. Massmann, *J. Appl. Phys.* **53**, 3237 (1982).
- ⁸G. C. Cho, W. Kütt, and H. Kurz, *Phys. Rev. Lett.* **65**, 764 (1990).
- ⁹T. K. Cheng, J. Vidal, H. J. Zeiger, G. Dresselhaus, M. S. Dresselhaus, and E. P. Ippen, *Appl. Phys. Lett.* **59**, 1923 (1991).
- ¹⁰J. M. Chwalek, C. Uher, J. F. Whitaker, and G. A. M. J. A. Agostinelli, *Appl. Phys. Lett.* **58**, 980 (1991).
- ¹¹Y. Tsay, B. Bendow, and S. S. Mitra, *Phys. Rev. B* **8**, 2688 (1973).
- ¹²K. L. Lewis, I. T. Muirhead, A. M. Pitt, A. G. Cullis, N. G. Chew, A. Miller, and T. J. Wyatt-Davies, *Appl. Opt.* **28**, 2785 (1989).
- ¹³Y. T. Chow, B. S. Wherrett, E. Van Stryland, B. T. McGuckin, D. Hutchings, J. G. H. Mathew, A. Miller, and K. Lewis, *J. Opt. Soc. Am. B* **3**, 1535 (1986).
- ¹⁴G. S. Buller (private communication).
- ¹⁵M. Sheik-Bahae, D. C. Hutchings, D. J. Hagan, and E. W. Van Stryland, *IEEE J. Quantum Electron.* **QE-27**, 1296 (1991).
- ¹⁶E. J. Canto-Said, D. J. Hagan, J. Young, and E. W. Van Stryland, *IEEE J. Quantum Electron.* **QE-27**, 2274 (1991).
- ¹⁷Landolt-Börstein, *Numerical Data and Functional Relationships in Science and Technology* (Springer, Berlin, 1982), Vols. 17a and 17b of Group III.
- ¹⁸S. Musikant, *Optical Materials: An Introduction to Selection and Application* (Marcel Dekker, New York, 1985).
- ¹⁹Y. Silberberg, P. W. Smith, D. A. B. Miller, B. Tell, A. C. Gossard, and W. Wiegmann, *Appl. Phys. Lett.* **46**, 701 (1985).
- ²⁰W. H. Knox, G. E. Doran, M. Asom, G. Livescu, R. Leibenguth, and S. N. G. Chu, *Appl. Phys. Lett.* **59**, 1491 (1991).